Computer Assisted Mechanics and Engineering Sciences, **10**: 531–543, 2003.


# Hybrid equilibrium plate elements of high degree

Edward A.W. Maunder
*Department of Engineering, School of Engineering, Computer Science and Mathematics, University of Exeter,*
*Harrison Building, North Park Road, Exeter, Devon, EX4 4QF, UK*

(Received September 11, 2003)

This paper concerns the modelling of plate bending problems governed by Reissner-Mindlin theory when hybrid equilibrium elements of high polynomial degree are used. The fields of statically admissible stress-resultants are categorised into three types according to the nature of their incompatibilities, i.e. pure Trefftz or strongly compatible, weakly compatible, and hyperstatic or strongly incompatible. The effects of this categorisation are reflected in the element formulation. Incompatibilities are quantified in terms of local discontinuities which also account for transverse twist terms. The construction of bases for the three corresponding subspaces of stress-resultants by numerical and/or algebraic means is reviewed. The potential use of a reformulated element is considered in the context of glass plate structures where residual or hyperstatic stresses play an important role.

## 1. Introduction

The modelling of thin plate bending problems with finite element techniques has spawned many different types of elements to cater for the special problems of simulating 3D structures as thin plates. Developments with stress based elements in hybrid forms have proved useful as an alternative, or a complement, to more conventional forms based on displacement fields [1]. Hybrid elements with discontinuous boundary displacements can enable models to satisfy completely the equilibrium conditions in a strong sense. This enables important bounded properties to be achieved, e.g. in the context of error estimation and limit analyses. A special case of stress based hybrids occurs when the internal fields are Trefftz functions [2, 3]. In this case internal stress fields are not only statically admissible but also kinematically admissible.

The existence of stress fields with different characteristics raises a question of choice and suitability for specific problems. It would seem useful to recognise special characteristics at the stage of element formulation rather than treat all stress fields in a similar way. A new formulation of hybrid equilibrium plate elements is proposed in this paper based on polynomial fields of general degree. This formulation is considered from a Trefftz perspective, and the fields of stress-resultants are categorised as (a) strongly compatible i.e. pure Trefftz, (b) weakly compatible, and (c) hyperstatic and hence strongly incompatible i.e. non-Trefftz.

The aims of such a formulation are to assist the study of the suitability of each category for problems driven by different types of excitation, e.g. loads, displacements, and initial strains; and to assist the study of compatibility defaults [4] as indicators of the local quality of solutions.

The paper proceeds with the following structure: Section 2 recapitulates the formulation of the hybrid equilibrium element, and Section 3 presents the vector space of internal stress-resultant fields as a decomposition into a direct sum of three subspaces which correspond to the above categorisation. Section 4 defines compatibility conditions and incompatibilities, from a local viewpoint, corresponding to initial "strains" and statically admissible fields of stress-resultants which include the Trefftz fields. Section 5 then reviews numerical and algebraic procedures for constructing bases for the three subspaces. The problem of modelling glass plate structures is discussed in Section 6

as an application where residual stresses are of great importance, and the paper is concluded in Section 7.

## 2. Formulation of the hybrid element

The formulation of the hybrid element is presented for completeness. It is based on polynomial fields of degree $p$ which are complete for side displacements,

$$\{\delta\} = [\mathbf{V}]\{\mathbf{v}\} \tag{1}$$

and for internal stress-resultants as far as statical admissibility allows. Statically admissible stress-resultants are represented by

$$\{\sigma\} = [\mathbf{S}]\{\mathbf{s}\}, \tag{2}$$

where the columns of $[\mathbf{S}]$ in Eq. (2) are basis functions for the vector space $\Sigma_{SA}$. The vector space $\Sigma_{SA}$ has an inner product defined for the domain $\Omega$ of an element:

$$\langle \sigma_1, \sigma_2 \rangle = \int_\Omega \{\sigma_1\}^{\mathrm{T}} [\mathbf{f}] \{\sigma_2\} \, \mathrm{d}\Omega \quad \text{and} \quad [\mathbf{f}]\{\sigma\} = \{\varepsilon\}, \tag{3}$$

where $\{\sigma\}$ is a vector of stress-resultants which contains three moment and two shear force components. $\{\varepsilon\}$ is the corresponding vector of deformations or strain-resultants.

The element equations take the form:

$$\begin{bmatrix} -\mathbf{F} & \mathbf{D}^{\mathrm{T}} \\ \mathbf{D} & \mathbf{0} \end{bmatrix} \begin{Bmatrix} \mathbf{s} \\ \mathbf{v} \end{Bmatrix} = \begin{Bmatrix} \overline{\mathbf{e}} \\ \overline{\mathbf{g}} \end{Bmatrix}, \tag{4}$$

where

$$[\mathbf{F}] = \int_\Omega [\mathbf{S}]^{\mathrm{T}} [\mathbf{f}] [\mathbf{S}] \, \mathrm{d}\Omega; \quad [\mathbf{D}] = \oint_\Gamma [\mathbf{V}]^{\mathrm{T}} [\overline{\mathbf{S}}] \, \mathrm{d}\Gamma; \quad \{\overline{\mathbf{e}}\} = \int_\Omega [\mathbf{S}]^{\mathrm{T}} \{\overline{\varepsilon}\} \, \mathrm{d}\Omega; \quad \{\overline{\mathbf{g}}\} = \oint_\Gamma [\mathbf{V}]^{\mathrm{T}} \{\overline{\mathbf{t}}\} \, \mathrm{d}\Gamma$$

and $[\overline{\mathbf{S}}]$ contains the side tractions equilibrating with $[\mathbf{S}]$. In this case the problem is driven by specified tractions $\{\overline{\mathbf{t}}\}$ and initial strains $\{\overline{\varepsilon}\}$. Body force and pressure loads are not considered in this paper.

The matrix transformations represent mappings between vector spaces as indicated in Fig. 1. Spaces $\Sigma_{\mathrm{SA}}$ and $E$ have dimension $n_s$ and $E$ contains the generalised strains $\{e\}$; spaces $G$ and $\Delta$ have dimension $n_v$ and they contain the modes of side traction and side displacement respectively. Subspaces $\Sigma_{\mathrm{HYP}}$ and $\Delta_K$ are the nullspaces of the equilibrium and compatibility maps, and they have dimensions denoted by $n_{\mathrm{hyp}}$ and $n_k$ respectively. Subspaces $G_{\mathrm{ADM}}$ and $E_{\mathrm{COM}}$ contain admissible tractions and compatible generalised strains as the ranges of the equilibrium and compatibility maps, their dimensions are denoted by $n_a$ and $n_c$ respectively.

Consistency of Eqs. (4) requires the tractions to be admissible, i.e.

$$[\mathbf{A}]^{\mathrm{T}} \{\overline{\mathbf{g}}\} = \{\mathbf{0}\}. \tag{5}$$

Compatibility of generalised initial strains requires that:

$$[\mathbf{B}]^{\mathrm{T}} \{\overline{\mathbf{e}}\} = \{\mathbf{0}\}, \tag{6}$$

where matrices $[\mathbf{A}]$ and $[\mathbf{B}]$ represent bases for the nullspaces $\Delta_K$ and $\Sigma_{\mathrm{HYP}}$ respectively.

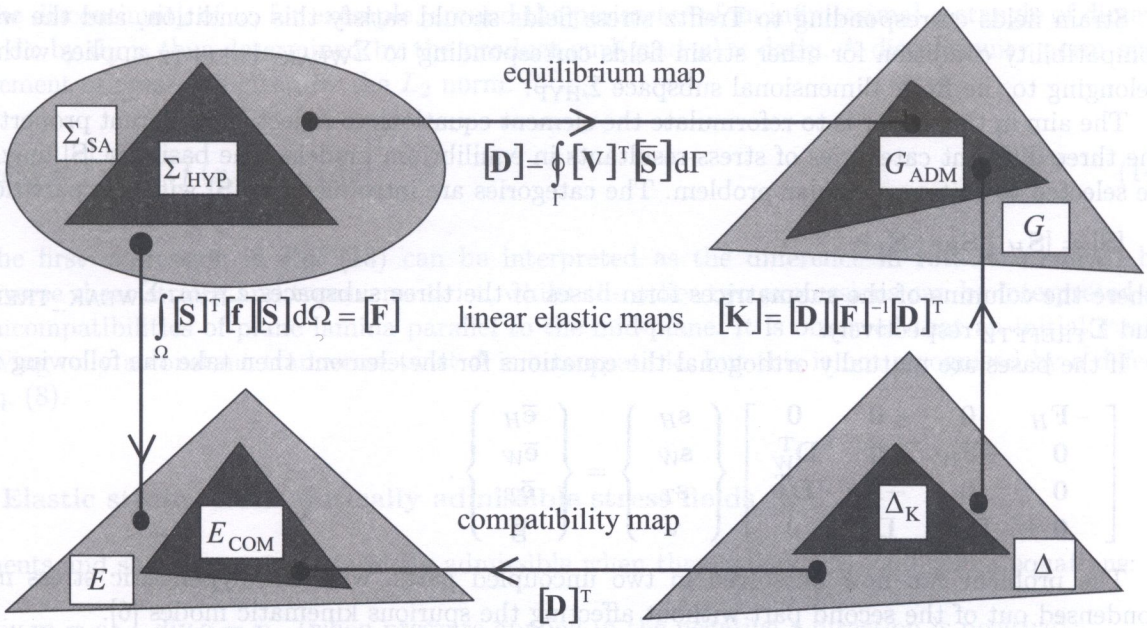


**Fig. 1.** Mappings between spaces

## 3. Decomposition of $\Sigma_{SA}$

The overall vector space $\Sigma_{SA}$ is now considered as the direct sum:

$$\Sigma_{SA} = \Sigma_{HYP} \oplus \Sigma_{WEAK\_TREFFTZ} \oplus \Sigma_{TREFFTZ}, \tag{7}$$

where 'HYP' refers to the subspace of hyperstatic stress fields, 'TREFFTZ' refers to the subspace of stress fields with fully compatible elastic deformations, and 'WEAK_TREFFTZ' refers to the direct complement of $\Sigma_{TREFFTZ} \oplus \Sigma_{HYP}$ in $\Sigma_{SA}$ whose stress fields satisfy some compatibility conditions by virtue of being orthogonal to the hyperstatic fields in $\Sigma_{HYP}$. The subspaces are shown diagrammatically in Fig. 2.

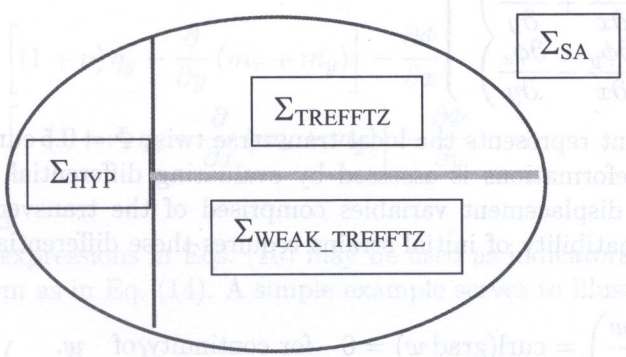


**Fig. 2.** Subspaces of the space of stress-resultants

The compatibility condition for arbitrary strain-resultants within an element can be expressed in the integral form using the principle of virtual work [5] as in Eq. (8)

$$\int_\Omega \{\sigma\}^T \{\varepsilon\}\, d\Omega = 0 \quad \text{for all possible hyperstatic stress fields } \{\sigma\}. \tag{8}$$

Strain fields corresponding to Trefftz stress fields should satisfy this condition, and the weaker compatibility condition for other strain fields corresponding to $\Sigma_{\text{WEAK\_TREFFTZ}}$ applies with $\{\boldsymbol{\sigma}\}$ belonging to the finite dimensional subspace $\Sigma_{\text{HYP}}$.

The aim in this paper is to reformulate the element equations to reflect the different properties of the three different categories of stress-resultants in equilibrium models. The basis for [**S**] may then be selected to suit a particular problem. The categories are introduced in [**S**] with the partition:

$$[\mathbf{S}] = [\mathbf{S}_H \mid \mathbf{S}_W \mid \mathbf{S}_T], \tag{9}$$

where the columns of the submatrices form bases of the three subspaces $\Sigma_{\text{HYP}}$, $\Sigma_{\text{WEAK\_TREFFTZ}}$, and $\Sigma_{\text{TREFFTZ}}$ respectively.

If the bases are mutually orthogonal the equations for the element then take the following form:

$$\begin{bmatrix} -\mathbf{F}_H & \mathbf{0} & \mathbf{0} & \mathbf{0} \\ \mathbf{0} & -\mathbf{F}_W & \mathbf{0} & \mathbf{D}_W^{\mathrm{T}} \\ \mathbf{0} & \mathbf{0} & -\mathbf{F}_T & \mathbf{D}_T^{\mathrm{T}} \\ \mathbf{0} & \mathbf{D}_W & \mathbf{D}_T & \mathbf{0} \end{bmatrix} \begin{Bmatrix} \mathbf{s}_H \\ \mathbf{s}_W \\ \mathbf{s}_T \\ \mathbf{v} \end{Bmatrix} = \begin{Bmatrix} \overline{\mathbf{e}}_H \\ \overline{\mathbf{e}}_W \\ \overline{\mathbf{e}}_T \\ \overline{\mathbf{g}} \end{Bmatrix}. \tag{10}$$

The problem can now be solved in two uncoupled parts, with the hyperstatic stress modes condensed out of the second part without affecting the spurious kinematic modes [6].

## 4. Compatibility conditions

### 4.1. Initial strains

Initial strains or deformations for the Reissner–Mindlin plate are described in terms of gradients of rotations of transverse sections $\boldsymbol{\phi}$ and equivalent transverse shear strains $\overline{\boldsymbol{\gamma}}$. The basic kinematic assumption for Reissner–Mindlin theory [7] is that the equivalent shear strains over a cross-section are defined by $\overline{\boldsymbol{\gamma}} = \boldsymbol{\phi} + \operatorname{grad} w$. The gradients of the components of $\boldsymbol{\phi}$ constitute the curvatures and the twists, defined as follows:

$$\begin{Bmatrix} \kappa_x \\ \kappa_y \\ \kappa_{xy} \\ \Phi \end{Bmatrix} = \begin{Bmatrix} \dfrac{\partial \phi_x}{\partial x} \\ \dfrac{\partial \phi_y}{\partial y} \\ \dfrac{1}{2}\left(\dfrac{\partial \phi_y}{\partial x} + \dfrac{\partial \phi_x}{\partial y}\right) \\ \dfrac{1}{2}\left(\dfrac{\partial \phi_y}{\partial x} - \dfrac{\partial \phi_x}{\partial y}\right) \end{Bmatrix}, \tag{11}$$

where the last component represents the local transverse twist $\Phi = 0.5 \operatorname{curl} \phi$ [8].

Incompatibility of deformations is assessed by evaluating differential expressions for discontinuities of the primary displacement variables comprised of the transverse deflection $w$ and the rotations $\boldsymbol{\phi}$. Then compatibility of initial strains requires these differential expressions to be zero. For example

$$\frac{\partial}{\partial x}\left(\frac{\partial w}{\partial y}\right) - \frac{\partial}{\partial y}\left(\frac{\partial w}{\partial x}\right) = \operatorname{curl}(\operatorname{grad} w) = 0 \quad \text{for continuity of} \quad w. \tag{12}$$

Then the discontinuities per unit area of the primary displacement variables can be expressed:

$$\begin{aligned} \overline{f}(x,y) &= \operatorname{curl}(\operatorname{grad} w) = \operatorname{curl} \overline{\boldsymbol{\gamma}} - 2\Phi, \\ \overline{g}(x,y) &= \operatorname{curl}(\operatorname{grad} \phi_x) = \frac{\partial}{\partial x}(\kappa_{xy} - \Phi) - \frac{\partial \kappa_x}{\partial y}, \\ \overline{h}(x,y) &= \operatorname{curl}(\operatorname{grad} \phi_y) = \frac{\partial \kappa_y}{\partial x} - \frac{\partial}{\partial y}(\kappa_{xy} + \Phi). \end{aligned} \tag{13}$$

The discontinuity of $w$, for example, around the perimeter of an infinitesimal rectangle of dimensions $\mathrm{d}x$ by $\mathrm{d}y$ is thus determined by the product $\mathrm{curl}(\mathrm{grad}\, w) \times \mathrm{d}x\mathrm{d}y$. A discontinuity norm over an element of area $A$ is given by the $L_2$ norm:

$$\|\widetilde{w}\|_2 = \left[\frac{1}{A}\int_A \left(\overline{f}\,(x,y)\right)^2 \mathrm{d}x\mathrm{d}y\right]^{1/2}. \tag{14}$$

The first expression in Eq. (13) can be interpreted as the difference in rotations caused by transverse shear strains and transverse twist, whilst the other two expressions can be interpreted as the incompatibilities of plane lamina parallel to the mid-plane. It is observed that an initial strain involving only a constant transverse twist $\Phi$ is incompatible, but this is not recognised by a defect in Eq. (8).

### 4.2. Elastic strains from statically admissible stress fields

Moments and shear forces are statically admissible when they satisfy the equilibrium equations:

$$\begin{aligned} &\mathrm{div}\,\mathbf{m} = q\,; \quad \mathrm{div}\,\mathbf{q} = p \quad \text{(when pressure applied in the negative } z \text{ direction is positive)}\,; \\ &\text{or combining the two equations:} \quad \mathrm{div}(\mathrm{div}\,\mathbf{m}) = p. \end{aligned} \tag{15}$$

In the absence of pressure or body forces, $p = 0$.

The elastic strain-resultants corresponding to a field of statically admissible stress-resultants lead to alternative forms of expressions for discontinuities after exploiting the equilibrium equations and the constitutive relations. Then

$$\begin{aligned} \mathrm{curl}(\mathrm{grad}\, w) &= \frac{12}{Gt}\mathrm{curl}\, q - 2\Phi, \\ \mathrm{curl}(\mathrm{grad}\, \phi_x) &= \frac{1}{2}\frac{\partial}{\partial x}\left[\frac{24\,(1+\nu)}{Et^3}m_{xy} - 2\Phi\right] - \frac{12}{Et^3}\frac{\partial}{\partial y}\left(m_x - \nu m_y\right), \\ \mathrm{curl}(\mathrm{grad}\, \phi_y) &= -\frac{1}{2}\frac{\partial}{\partial y}\left[\frac{24\,(1+\nu)}{Et^3}m_{xy} + 2\Phi\right] + \frac{12}{Et^3}\frac{\partial}{\partial x}\left(m_y - \nu m_x\right) \end{aligned} \tag{16}$$

and the last two expressions can be simplified to

$$\begin{aligned} \mathrm{curl}(\mathrm{grad}\, \phi_x) &= \frac{12}{Et^3}\left[(1+\nu)\, q_y - \frac{\partial}{\partial y}\left(m_x + m_y\right)\right] - \frac{\partial \Phi}{\partial x}, \\ \mathrm{curl}(\mathrm{grad}\, \phi_y) &= \frac{12}{Et^3}\left[-(1+\nu)\, q_x + \frac{\partial}{\partial x}\left(m_x + m_y\right)\right] - \frac{\partial \Phi}{\partial y}, \end{aligned} \tag{17}$$

where $\Phi$ is undetermined.

The residuals of the expressions in Eqs. (16) may be used as indicators of incompatibility error together with an $L_2$ norm as in Eq. (14). A simple example serves to illustrate. Consider:

$$\{\sigma\} = \begin{Bmatrix} m_x \\ m_y \\ m_{xy} \\ q_x \\ q_y \end{Bmatrix} = \begin{Bmatrix} 0 \\ 0 \\ -1.5y^2 \\ -3y \\ 0 \end{Bmatrix}. \tag{18}$$

This field is statically admissible with zero transverse pressure $p$. Although $\Phi$ is undetermined it may be included so as to eliminate either transverse or in-plane discontinuities. With transverse

continuity imposed, $\Phi = \dfrac{0.6}{Gt} \cdot \operatorname{curl} \mathbf{q} = \dfrac{1.8}{Gt}$ since $\operatorname{curl} \mathbf{q} = 3$, and then the in-plane discontinuities are quantified by Eq. (17) as a 2D vector.

$$\frac{12}{Et^3} \begin{Bmatrix} 0 \\ 3(1+\nu)\, y \end{Bmatrix} \quad [\mathrm{rad/m^2}]. \tag{19}$$

Alternatively if in-plane continuity is imposed, then from Eq. (17)

$$\operatorname{grad} \Phi = \frac{12}{Et^3} \begin{Bmatrix} 0 \\ 3(1+\nu)\, y \end{Bmatrix} \quad \text{or} \quad \Phi = \frac{18(1+\nu)}{Et^3} \cdot y^2 + \text{ a constant.} \tag{20}$$

Then the local transverse discontinuity is determined to within a constant as:

$$\operatorname{curl}(\operatorname{grad} w) = -\frac{36(1+\nu)}{Et^3} \cdot y^2 \quad [\mathrm{rad/m^2}]. \tag{21}$$

Another example is provided by a triangular element with the 4th degree hyperstatic field of stress-resultants specified in Eq. (22).

$$\begin{Bmatrix} m_x \\ m_y \\ m_{xy} \end{Bmatrix} = \frac{1}{ab} \begin{Bmatrix} \dfrac{x^4}{b^2} + \dfrac{6x^3y}{ab} + \dfrac{6x^2y^2}{a^2} - \dfrac{2x^3}{b} - \dfrac{6x^2y}{a} + x^2 \\ \dfrac{6x^2y^2}{b^2} + \dfrac{6xy^3}{ab} + \dfrac{y^4}{a^2} - \dfrac{6xy^2}{b} - \dfrac{2y^3}{a} + y^2 \\ \dfrac{-4x^3y}{b^2} - \dfrac{9x^2y^2}{ab} + \dfrac{6x^2y}{b} - \dfrac{4xy^3}{a^2} + \dfrac{6xy^2}{a} - 2xy \end{Bmatrix}. \tag{22}$$

This moment field has zero shear forces, and contravariant components are given with reference to the skew axes indicated in Fig. 3. The dimensions $a$ and $b$ refer to the lengths of two sides of the triangle. Figure 3 includes a plot of principal moment crosses evaluated at a set of uniformly spaced gridpoints. The details are derived in [9]. Figure 4 illustrates the distribution of the discontinuity vector at the same gridpoints after imposing transverse continuity.

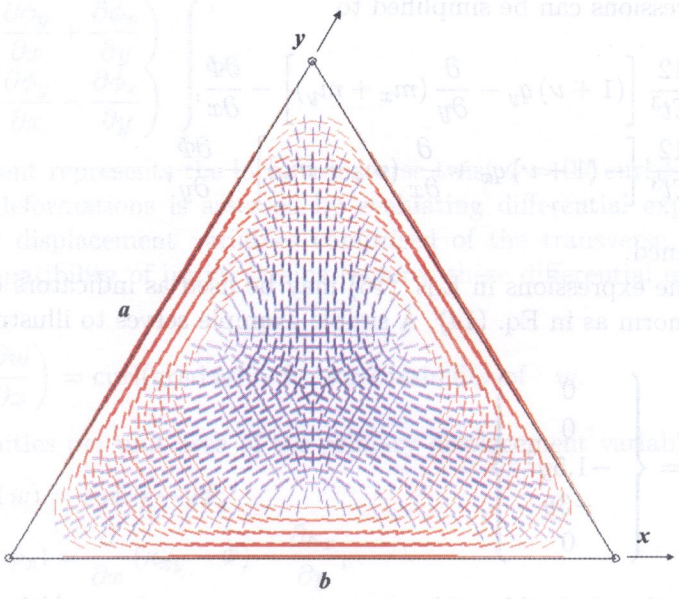


**Fig. 3.** Principal moment trajectories for the 4th degree hyperstatic field in Eq. (22)

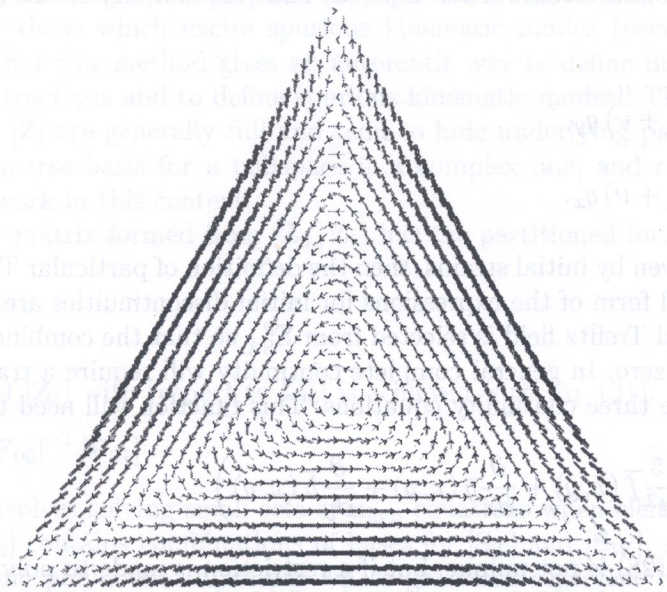

**Fig. 4.** Vector plot of in-plane lamina discontinuities from the moment field in Eq. (22)

### 4.3. Trefftz fields of stress-resultants

Stress-resultants belonging to $\Sigma_{\text{TREFFTZ}}$ are fully compatible and thus the discontinuities of their strains must be zero. Considering first zero transverse discontinuity:

$$2\Phi = \operatorname{curl} \overline{\gamma} = \frac{1.2}{Gt} \operatorname{curl} \mathbf{q} = 0. \tag{23}$$

This condition leads (see Appendix) to the form of Helmholz Eq. (24) for a uniform isotropic plate:

$$\left[\nabla^2 - \frac{10}{t^2}\right] \operatorname{curl} \mathbf{q} = 0\,, \quad \text{or} \quad \left[\nabla^2 - \frac{10}{t^2}\right] \Phi = 0. \tag{24}$$

Then the conditions for zero in-plane discontinuity form Eq. (25):

$$\begin{aligned} \frac{\partial}{\partial y}(m_x + m_y) &= (1+\nu)\left[q_y - \frac{t^2}{10}\frac{\partial \operatorname{curl} \mathbf{q}}{\partial x}\right], \\ \frac{\partial}{\partial x}(m_y + m_x) &= (1+\nu)\left[q_x + \frac{t^2}{10}\frac{\partial \operatorname{curl} \mathbf{q}}{\partial y}\right]. \end{aligned} \tag{25}$$

The compatibility conditions are collected together in Eq. (26).

$$\left[\begin{array}{ccc|cc} 0 & 0 & 0 & -\left[\nabla^2 - \dfrac{10}{t^2}\right]\dfrac{\partial}{\partial y} & \left[\nabla^2 - \dfrac{10}{t^2}\right]\dfrac{\partial}{\partial x} \\ -\dfrac{\partial}{\partial y} & -\dfrac{\partial}{\partial y} & 0 & +\dfrac{(1+\nu)\,t^2}{10}\dfrac{\partial^2}{\partial x \partial y} & -\dfrac{(1+\nu)\,t^2}{10}\left[\dfrac{\partial^2}{\partial x^2} - \dfrac{10}{t^2}\right] \\ \dfrac{\partial}{\partial x} & \dfrac{\partial}{\partial x} & 0 & +\dfrac{(1+\nu)\,t^2}{10}\left[\dfrac{\partial^2}{\partial y^2} - \dfrac{10}{t^2}\right] & -\dfrac{(1+\nu)\,t^2}{10}\dfrac{\partial^2}{\partial x \partial y} \end{array}\right] \left\{\begin{array}{c} m_x \\ m_y \\ m_{xy} \\ q_x \\ q_y \end{array}\right\} = \left\{\begin{array}{c} 0 \\ 0 \\ 0 \end{array}\right\}. \tag{26}$$

In the case of polynomial Trefftz fields Eq. (23) and (25) simplify to the set in Eq. (27).

$$\begin{aligned} &\operatorname{curl} \mathbf{q} = 0, \\ &\frac{\partial}{\partial y}(m_x + m_y) = (1+\nu)\, q_y, \\ &\frac{\partial}{\partial x}(m_y + m_x) = (1+\nu)\, q_x. \end{aligned} \tag{27}$$

If the problem is driven by initial strains, then the definition of particular Trefftz fields needs to be considered. The general form of the expressions for initial discontinuities are contained in Eq. (13). A particular polynomial Trefftz field is selected from $\Sigma_{\mathrm{SA}}^{p}$ so that the combined discontinuities from Eqs. (13) and (16) are zero. In general complete continuity will require a transverse twist function $\Phi$ for consistency of the three continuity equations. This function will need to satisfy Eq. (28).

$$\left[\nabla^2 - \frac{10}{t^2}\right] \Phi = \left( -\frac{5}{t^2}\overline{f}\,(x,y) + \frac{\partial}{\partial x}\overline{g}\,(x,y) + \frac{\partial}{\partial y}\overline{h}\,(x,y) \right). \tag{28}$$

The solution to Eq. (28) is not unique, but if a restriction is made to polynomial functions, then $\Phi$ can be simply determined and then a particular field of stress-resultants can be selected. Only when the right hand side of Eq. (28) is zero will the discontinuities be consistent without the need for introducing transverse twist.

## 5. Bases for $\Sigma_{\mathrm{SA}}$

The construction of these bases may be carried out in a number of ways. Two constructions are considered here, a general numerical procedure, and a procedure which exploits a mix of general algebraic forms and some numerical procedures. In either procedure the process starts from an arbitrary basis for $\Sigma_{\mathrm{SA}}$, and this may be simply derived for example from a set of Southwell functions complete to some degree. General properties of bases for $\Sigma_{\mathrm{TREFFTZ}}$ and $\Sigma_{\mathrm{HYP}}$ which may be recognised *ab initio* are:

$[\mathbf{S}_T]$ is independent of the element shape or size, and generates a subspace in its own right;

$[\mathbf{S}_H]$ is dependent on the element shape and size, and generates a subspace in its own right which is orthogonal to $[\mathbf{S}_T]$.

### 5.1. Numerical procedures

The mapping from fields of stress-resultants to admissible side tractions is represented by the $n_v \times n_s$ matrix $[\mathbf{D}]$. Singular value decomposition [10] of this matrix yields Eq. (29).

$$[\mathbf{Y}]^{\mathrm{T}}\,[\mathbf{D}]\,[\mathbf{Z}] = [\mathbf{W}] \quad \text{or} \quad [\mathbf{D}]\,\{\mathbf{z}_i\} = \mathbf{w}_i\,\{\mathbf{y}_i\}, \tag{29}$$

where $[\mathbf{W}]$ contains the singular values $\mathbf{w}_i$ of $[\mathbf{D}]$ on its diagonal, and the columns of $[\mathbf{Z}]$ and $[\mathbf{Y}]$ represent internal stress-resultant and side traction vectors respectively. The columns of $[\mathbf{Z}]$ are partitioned into a right hand set of $n_{\mathrm{hyp}}$ columns $[\mathbf{Z}_0]$ which represent a basis for $\Sigma_{\mathrm{HYP}}$, and a left hand set of $n_a = n_s - n_{\mathrm{hyp}}$ columns $[\mathbf{Z}_1]$ which represent a basis for a direct complement of $\Sigma_{\mathrm{HYP}}$ in $\Sigma_{\mathrm{SA}}$. However these bases are not necessarily orthogonal to each other with respect to the inner product defined in Eq. (3), and thus Trefftz fields are unlikely to be explicitly determined by this decomposition.

The columns of $[\mathbf{Y}]$ are partitioned into a right hand set of $n_a$ admissible tractions, each of which is equilibrated by a particular field of stress-resultants corresponding to a vector in $[\mathbf{Z}]$, and

a set of $n_k = n_v - n_a$ inadmissible tractions. Inadmissible tractions are those which are not in overall equilibrium, or those which excite spurious kinematic modes (pseudo mechanisms). The useful feature here is that this method gives an automatic way to define internal stress-resultants in terms of admissible tractions and to define spurious kinematic modes!! The disadvantage is that the vectors in $[\mathbf{Y}]$ and $[\mathbf{Z}]$ are generally full and tend to hide underlying patterns or sparsity. The problem of finding a sparse basis for a nullspace is a complex one, and reference may be made to [11, 12] for further work in this context.

A natural flexibility matrix formed from $[\mathbf{Z}_0 \,|\, \mathbf{Z}_1]$ has the partitioned form in Eq. (30).

$$[\mathbf{F}] = \begin{bmatrix} \mathbf{F}_{00} & \mathbf{F}_{01} \\ \mathbf{F}_{10} & \mathbf{F}_{11} \end{bmatrix}. \tag{30}$$

Orthogonalisation of $[\mathbf{Z}_1]$ with respect to $[\mathbf{Z}_0]$ is achieved with Eq. (31).

$$[\mathbf{Z}_2] = [\mathbf{Z}_1] - [\mathbf{Z}_0]\,[\mathbf{F}_{00}]^{-1}\,[\mathbf{F}_{01}]\,. \tag{31}$$

This change only involves solving small sets of $\mathbf{n}_{\text{hyp}}$ equations when elements are of low degree. The orthogonal set $[\mathbf{Z}_2]$ contains combinations of bases for $[\mathbf{S}_T]$ and $[\mathbf{S}_W]$. A basis for $[\mathbf{S}_T]$ can be derived from biharmonic polynomial functions whose gradients represent rotation fields $\phi$ [3], or from enforcing the continuity conditions on a basis for $\Sigma_{\text{SA}}$ [13].

The last set of stress-resultants $[\overline{\mathbf{S}}_W]$ is contained within $[\mathbf{Z}_2]$ and these can be selected by invoking the Exchange Theorem [14]. At this stage the natural flexibility matrix has the partitioned form in Eq. (32).

$$[\mathbf{F}] = \begin{bmatrix} \mathbf{F}_{00} & 0 & 0 \\ 0 & \overline{\mathbf{F}}_W & \mathbf{F}_{WT} \\ 0 & \mathbf{F}_{TW} & \mathbf{F}_T \end{bmatrix}. \tag{32}$$

Finally $[\overline{\mathbf{S}}_W]$ is orthogonalised with respect to $[\mathbf{S}_T]$ by combining as in Eq. (33).

$$[\mathbf{S}_W] = [\overline{\mathbf{S}}_W] - [\mathbf{S}_T]\,[\mathbf{F}_T]^{-1}\,[\mathbf{F}_{TW}]\,. \tag{33}$$

This method is perhaps rather heavyweight in terms of computational effort. The other approach takes advantage of bases which can be defined *a priori* by a direct algebraic analysis.

### 5.2. Algebraic procedures

A basis for $\Sigma_{\text{HYP}}$ can be formed by enforcing the zero equilibrating traction condition on the sides of an element. The enforcement is simplified for a triangular element by using oblique axes parallel with two sides of a triangle, and by using contragredient components of stress-resultants. This is described in more detail in [9].

A basis for $\Sigma_{\text{TREFFTZ}}$ can be derived algebraically as before. By definition, the bases for $\Sigma_{\text{HYP}}$ and $\Sigma_{\text{TREFFTZ}}$ are orthogonal, and it remains to complete a basis for $\Sigma_{\text{SA}}$. This may be done again by exploiting the Exchange Theorem using the initial the basis formed from Southwell functions to obtain a set of independent incompatible stress-resultant fields $[\mathbf{S}_{NT}]$. The latter are not necessarily orthogonal to the hyperstatic fields. The basis for $\Sigma_{\text{SA}}$ at this stage appears in Eq. (34),

$$[\mathbf{S}] = [\ \mathbf{S}_H \,|\, \mathbf{S}_{NT} \,|\, \mathbf{S}_T\ ] \tag{34}$$

and the natural flexibility matrix has the form in Eq. (35).

$$[\mathbf{F}] = \begin{bmatrix} \mathbf{F}_H & \mathbf{F}_{HN} & 0 \\ \mathbf{F}_{NH} & \mathbf{F}_N & \mathbf{F}_{NT} \\ \mathbf{0} & \mathbf{F}_{TN} & \mathbf{F}_T \end{bmatrix}. \tag{35}$$

The incompatible fields in $[\mathbf{S}_{NT}]$ are then transformed into weakly compatible ones $[\overline{\mathbf{S}}_W]$ in Eq. (36),

$$[\overline{\mathbf{S}}_W] = [\mathbf{S}_{NT}] - [\mathbf{S}_H]\,[\mathbf{F}_H^{-1}]\,[\mathbf{F}_{HN}] \tag{36}$$

and finally $[\overline{\mathbf{S}}_W]$ is again orthogonalised with respect to $[\mathbf{S}_T]$ as in Eq. (33).

Algebraic results are illustrated for a triangular primitive plate element where the hyperstatic modes are present when $p \geq 4$. Table 1 shows the dimensions for the subspaces for the direct sum of $\Sigma_{SA}$. When $p = 8$ there is an approximate balance between the three dimensions, and for higher degrees the hyperstatic fields dominate due to the dependence on the square of $p$. The other two subspaces are only linearly dependent on $p$.

**Table 1.** Dimensions of spaces of statically admissible fields of stress-resultants for a triangle.

| Degree $p$ of moments | $n_s$ | $n_{\text{hyp}}$ | $n_{\text{weak\_T}}$ | $n_{\text{T}}$ |
|---|---|---|---|---|
| 0 | 3 | 0 | 0 | 3 |
| 1 | 9 | 0 | 2 | 7 |
| 2 | 17 | 0 | 6 | 11 |
| 3 | 27 | 0 | 12 | 15 |
| 4 | 39 | 3 | 17 | 19 |
| >4 | $(p^2 + 5p + 3)$ | $(p^2 - 4p + 3)$ | $(5p - 3)$ | $(4p + 3)$ |
| 8 | 107 | 35 | 37 | 35 |
| 10 | 153 | 63 | 47 | 43 |

One of the three hyperstatic fields when $p = 4$ is defined in Eq. (22), and illustrated in Fig. 3.

## 6. An application to glass plate structures

An application to a residual stress problem is considered in the context of glass plate structures where the prediction of high quality information on residual stress is important.

An early example of a residual stress problem was considered by J. C. Maxwell [15]. He referred to a number of problems to which he applied recent work on photoelasticity as an experimental method to verify theory. However his last problem concerned a triangular glass plate heated to a high temperature and rapidly cooled (e.g. quenched). This process produces residual stresses for which there was no theoretical solution. His photoelastic technique led to the production of the pattern of planar stress trajectories in Fig. 5. This should be compared with the hyperstatic stress field of 4th degree derived for the membrane aspect of the hybrid plate element [9]. This has exactly the same pattern as the stresses produced by the pure moment field defined in Eq. (22) and illustrated in Figs. 3 and 6. The 4th degree field is remarkably similar to that found by Maxwell and serves to demonstrate that such fields are relevant to residual stress problems!

A similar manufacturing process is currently used in the production of toughened and/or strengthened glass plates, the object being to induce compressive residual stresses at the surfaces so as to inhibit the propagation of cracks from within the plate to its surfaces [16]. Simulating the manufacturing process so as to predict and control such patterns or prestress appears to be another challenging problem.

The use of glass plates as structural components appears to be increasing [16] as illustrated in Fig. 7.

Typical features of glass structural behaviour appear to lend themselves to simulation by equilibrium models. These features include:

- Brittle material, designers cannot ignore stress concentrations;
- Elastic material behaviour which can involve large deflections with small strains, hence non-linear structural behaviour involving both bending and membrane actions;
- Loading from wind pressure et al, but also stressed by manufacturing processes and temperature gradients;
- Sensitivity to support conditions;
- Design criteria related to maximum principal stresses.

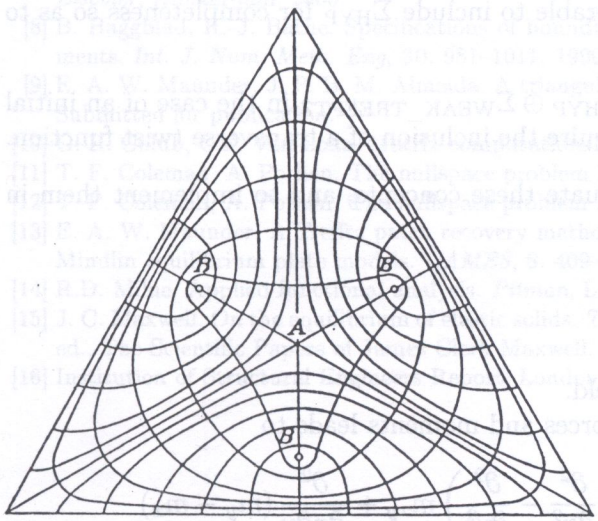


**Fig. 5.** Residual stress trajectories from photoelasticity [15]

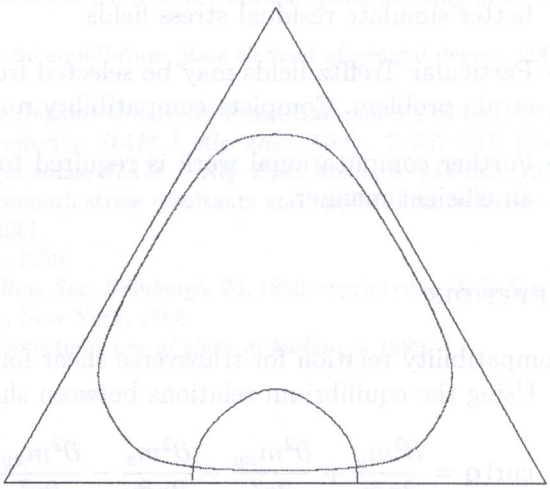

**Fig. 6.** Residual stress trajectories from Eq. (22) [9]

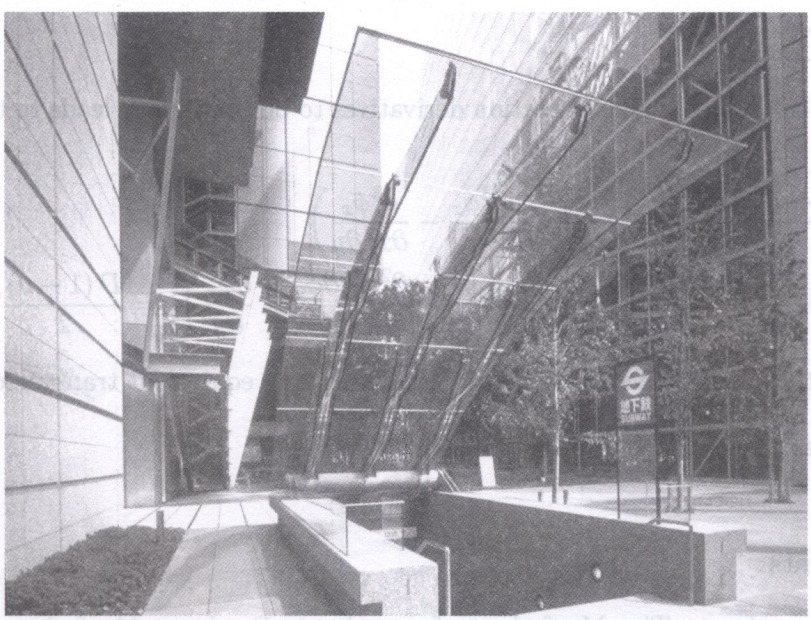

**Fig. 7.** The Yurakucho glass canopy, Tokyo

## 7. Conclusions

- The space of statically admissible stress-resultant fields within a hybrid element can be decomposed into a direct sum of three subspaces which are orthogonal with respect to the energy inner product;
- For load excitation, modelling with high degree elements becomes dominated by the hyperstatic subspace $\Sigma_{\text{HYP}}$. There is a need to weigh up the computational effort in including this subspace with the extra accuracy that may be achieved with it. $\Sigma_{\text{HYP}}$ can be excluded without any penalty from spurious kinematic modes, whereas the inclusion of $\Sigma_{\text{WEAK\_TREFFTZ}}$ is a way to supplement the Trefftz element with weakly compatible stress fields which avoid potential problems with spurious kinematic modes;
- For initial strain excitation, it would seem preferable to include $\Sigma_{\text{HYP}}$ for completeness so as to better simulate residual stress fields.
- Particular Trefftz fields may be selected from $\Sigma_{\text{HYP}} \oplus \Sigma_{\text{WEAK\_TREFFTZ}}$ in the case of an initial strain problem. Complete compatibility may require the inclusion of a transverse twist function.
- Further computational work is required to evaluate these concepts, and to implement them in an efficient manner.

## Appendix

Compatibility relation for transverse shear force field.

Using the equilibrium relations between shear forces and moments leads to

$$\operatorname{curl}\mathbf{q} = \frac{\partial^2 m_y}{\partial x \partial y} + \frac{\partial^2 m_{xy}}{\partial x^2} - \frac{\partial^2 m_x}{\partial x \partial y} - \frac{\partial^2 m_{xy}}{\partial y^2} = \left(\frac{\partial^2}{\partial x^2} - \frac{\partial^2}{\partial y^2}\right) m_{xy} + \frac{\partial^2}{\partial x \partial y}\left(m_y - m_x\right)$$

Using the constitute relations between moments and curvatures leads to

$$\operatorname{curl}\mathbf{q} = \frac{D\left(1-\nu\right)}{2}\left(\frac{\partial^2}{\partial x^2} - \frac{\partial^2}{\partial y^2}\right)\left(\frac{\partial \phi_x}{\partial y} + \frac{\partial \phi_y}{\partial x}\right) + D\frac{\partial^2}{\partial x \partial y}\left(\nu\frac{\partial \phi_x}{\partial x} + \frac{\partial \phi_y}{\partial y} - \frac{\partial \phi_x}{\partial x} - \nu\frac{\partial \phi_y}{\partial y}\right)$$

where $D = \dfrac{Et^3}{12\left(1-\nu^2\right)}$.

Assuming the components of the rotation derivatives to be continuous leads to the simplification of the expression for curl$\mathbf{q}$:

$$\begin{aligned}\operatorname{curl}\mathbf{q} &= \frac{D\left(1-\nu\right)}{2}\left(\frac{\partial^3 \phi_y}{\partial x^3} + \frac{\partial^3 \phi_y}{\partial x \partial y^2} - \frac{\partial^3 \phi_x}{\partial y^3} - \frac{\partial^3 \phi_x}{\partial x^2 \partial y}\right) \\ &= \frac{D\left(1-\nu\right)}{2}\left[\frac{\partial^2}{\partial x^2}\left(\frac{\partial \phi_y}{\partial x} - \frac{\partial \phi_x}{\partial y}\right) + \frac{\partial^2}{\partial y^2}\left(\frac{\partial \phi_y}{\partial x} - \frac{\partial \phi_x}{\partial y}\right)\right] = \frac{D\left(1-\nu\right)}{2}\nabla^2\left(\operatorname{curl}\phi\right).\end{aligned}$$

Finally using the constitutive relation between shears and equivalent transverse shear strains:

$$\operatorname{curl}\mathbf{q} = \frac{t^2}{10}\nabla^2\left(\operatorname{curl}\mathbf{q}\right).$$

### Acknowledgments

Grateful thanks are due to Tim Macfarlane of consultants Dewhurst Macfarlane & Partners, designers of the Yurakucho glass canopy, for supplying the photograph reproduced in Fig. 7.

## References


[1] J. P. Moitinho de Almeida, J. A. Teixeira de Freitas. Alternative approach to the formulation of hybrid equilibrium finite elements. *Computers and Structures*, **40**(4): 1043–1047, 1991.

[2] J. Jirousek, A. Wroblewski. T-elements: state of the art and future trends. *Arch. Comp. Meth. Engrg.*, **3/4**: 323–434, 1996.

[3] J. Jirousek, A. Wroblewski, Q.H. Qin, X.Q. He. A family of quadrilateral hybrid-Trefftz p-elements for thick plate analysis. *Comp. Meth. Appl. Mech. Engrg.*, **127**: 315–344, 1995.

[4] O. J. B. A. Pereira, J. P. M. Almeida, E. A. W. Maunder. Adaptive methods for hybrid equilibrium finite element models. *Comp. Meth. Appl. Mech. Eng*, **176**: 19–39, 1999.

[5] G. A. O. Davies. Virtual work in structural analysis. *Wiley*, Chichester, 1982.

[6] E. A. W. Maunder, J. P. Moitinho de Almeida, A. C. A. Ramsay. A general formulation of equilibrium macro-elements with control of spurious kinematic modes. *Int. J. Num Meth. Eng.*, **39**: 3175–3194, 1996.

[7] C. M. Wang, J. N. Reddy, K. H. Lee. Shear deformable beams and plates – Relationships with classical solutions. *Elsevier*, Amsterdam, 2000.

[8] B. Haggblad, K.-J. Bathe. Specifications of boundary conditions for Reissner-Mindlin plate bending finite elements. *Int. J. Num. Meth. Eng*, **30**: 981–1011, 1990.

[9] E. A. W. Maunder, J. P. B. M. Almeida. A triangular hybrid equilibrium plate element of general degree. 2003. Submitted for publication.

[10] G. H. Golub, C.F. Van Loan. Matrix computations. *Johns Hopkins University Press*, Baltimore, 3 edition, 1996.

[11] T. F. Coleman, A. Pothen. The nullspace problem I: Complexity. *SIAM J. Alg. Disc. Meth.*, **7**: 527–537, 1986.

[12] T. F. Coleman, A. Pothen. The nullspace problem II: Algorithms. *SIAM J. Alg. Disc. Meth.*, **8**: 544–563, 1987.

[13] E. A. W. Maunder. A Trefftz patch recovery method for smooth stress resultants and applications to Reissner-Mindlin equilibrium plate models. *CAMES*, **8**: 409–424, 2001.

[14] R.D. Milne. Applied functional analysis. *Pitman*, London, 1980.

[15] J. C. Maxwell. On the equilibrium of elastic solids. *Trans. Roy. Soc. Edinburgh*, 20, 1850. reprinted in W.D.Niven, ed., The Scientific Papers of James Clerk Maxwell. Dover, New York, 1965.

[16] Institution of Structural Engineers Report, London. *The structural use of glass in buildings*, 1999.